Mechanical Systems and Signal Processing 119 (2019) 589–602

Contents lists available at ScienceDirect

Mechanical Systems and Signal Processing

journal homepage: www.elsevier.com/locate/ymssp

Implementation of model-free motion control for active suspension systems

Jue Wang *, Fujiang Jin, Lichun Zhou, Ping Li

College of Information Science and Engineering, Huaqiao University, Xiamen 361021, China

ARTICLE INFO

Article history:
Received 18 July 2018
Received in revised form 11 September 2018
Accepted 5 October 2018
Available online 19 October 2018

Keywords:
Disturbance compensation
Model-free control
Motion control
Vehicle suspension systems

ABSTRACT

This paper focuses on the implementation of motion control for active suspension systems using a novel scheme of model-free finite-time tracking control method. The proposed strategy facilitates the realization since the system plant modeling is not needed. Correspondingly, the suspension vertical dynamics including external disturbances are estimated by the time-delay estimation, and its estimated error is compensated by the integral sliding mode control scheme. Theoretical analysis proves that the sliding mode and desired system dynamics can achieve a finite time convergence performance with continuous control law. In active suspension control, the continuous control law contributes to preventing the unexpected chattering in practical implementation. The advantage of the presented control algorithm is verified via comparative investigation, especially the comparison of the existing extended state observer-based feedback control scheme, which requires a high-gain observer to realize the desired dynamics. Comparative experimental studies are presented to confirm the effectiveness and superiority of the proposed control strategy over the traditional methods.

1. Introduction

In recent years, road vehicle safety concerns and performance have been regarded as a research focus since worldwide the road traffic fatalities claim a staggering 1.25 million lives annually and frequently cause approximate 50 million people suffering from non-fatal injuries [1]. Various researches of vehicle systems have received an almost identical conclusion that the vehicle suspension systems, which transmit the vibrations between the body and the irregular road surface, mainly determine the ride safety and maneuverability of an automobile [2–7]. Moreover, the suspension systems should also provide passengers with a high level of ride comfort to prevent physical fatigue while they enable the driver to maintain authority over the vehicle in critical situations. Due to the fact that the suspension systems have a significant impact on the subjective feelings of the vehicle, the customer raises increasingly requirements for modern automobiles to achieve the substantial performance improvements of safety and ride comfort. Therefore, the design of vehicle suspension systems are still needed further studies on these aspects, which represent a challenge to automotive industries, both in terms of science and engineering.

The active suspension system is unique of its own advantages among all types of the conventional vehicle suspension systems, such as passive or semi-active suspensions. To achieve a satisfactory active suspension control effect, an accurate mathematical description of its dynamic characteristic is required in general. According to the original suspension dynamics,

* Corresponding author.
E-mail address: xiaoyuwang@126.com (J. Wang).

https://doi.org/10.1016/j.ymssp.2018.10.004
0888-3270/

robust control [8,9], adaptive control [10–12], sliding mode control [13] and nonlinear frequency-domain method [14–16] have been applied in constructing control laws. However, the components of suspension are generally characterized by nonlinear, uncertainty and complex dynamics, it is difficult to accurately identify the parameters of the suspension models. Thus, model-based suspension control algorithm design is impractical under the imprecise and uncertain conditions. In order to avoid the identification of the suspension dynamic parameters, intelligent learning algorithms such as fuzzy logic controller and neural-network controller, have been introduced to establish the "black box" models of suspensions since their capabilities of nonlinear approximation. However, numerous learning parameters in the above mentioned methods limit their further application. Based upon the above analysis, it reveals that both the explicit and black-box mathematical models of the suspensions are only applicable to the experienced researchers since they require the complex algorithms at different stages of their implementation.

Recently, a robust control method by means of the extended state observer (ESO) was proposed in [17] to handel the plants with little model information in both system dynamics and external disturbances [18–22]. A significant advantage of these novel control structures are that they can regard the whole unknown system dynamics and disturbances of the plant as a generalized disturbance, which is estimated and compensated by an ESO in a feedforward way. The result of ESO shows that the main approach to improve the observation accuracy is using the high work bandwidth, which is a critical factor closely related to the cost in the industrial applications. Although the observation ability is increasing with the improving bandwidth, it leads to a series of problems, such as (1) the requirement for the improvement of the actuator quality; (2) the excitation of the complex dynamic problems in high frequency; (3) the reduction of stability margin for the closed-loop system, and more sensitive to the phase lag and time delay; (4) the high sensitivity to the noise in the sensors. Thus, there are few applications in the control engineering with high bandwidth and even high gain control laws. In addition, the residual estimate error of the ESO-based feedback controller presented in [21] is not addressed by active compensation. Thus, it can only achieve the bounded stability and, obviously, may not realize better performance.

To obtain a simple and reliable model-free method for control design purposes, the time-delay estimation (TDE) technique is considered as an attractive alternative [23,24]. By means of the time delay information, the robust time-delay control approach is proposed to approximate the unknown functions of system dynamics [25,26]. The existing time-delay control is constituted of two parts to deal with the unknown system, namely, combining a TDE with a linear controller. The TDE focuses on the estimation of the unknown model information, while the linear controller decides the desired closed-system performance. During the implementation process, all the unknown dynamic terms of the actual control plant are approximated through an estimate expression, which is described by the immediate past time instant information of the system state and control input. On the basis of this method, it is not difficult to reduce the tedious modelling complexity of the uncertain systems without loss of the precision of the model. Hence, the time-delay control approach has properties of model-free, simple structure and effective in general. However, the approximation errors, also called TDE errors, inevitably exist in its estimation process, which are regarded as the time-delayed errors/model uncertainties, have severe influence on the performance of the closed-loop systems. Thus, these model errors/uncertainties lead to the performance reduction of the presented control laws.

As a measure of uncertainty suppression, sliding mode control (SMC) performs excellent robustness performance [27–29]. However, the classical SMC has significant limitations, which restrict its practical application [30,31]. For instance, the classical SMC could not ensure the finite time convergence of the sliding surface when it comes to using a linear sliding surface. To overcome this obstacle, the terminal sliding mode control (TSMC) was proposed [32], which could guarantee the system to be finite-time stable using the nonlinear sliding surface to replace the original linear one. It is necessary to point out that the uncertainties might seriously affect the dynamic performances of the systems in the TSMC if the system states away from the equilibrium point. In recent years, the high-order sliding mode method is widely used in practice [33], especially super-twisting algorithm (STA), which also can be promised as a potential approach since it can preserve the main properties of the classical SMC while can also reduce the chattering. When the STA addresses the linearly growing perturbation, it also appears to be inadequate. Hence, a modified STA is presented to deal with the linear perturbation in [34], where the sliding mode switching gains are adjusted to obtain the rejection performance of disturbances.

Inspired by the above discussions, it is necessary to propose a model-free control scheme for active suspension systems. From a perspective of applied study, the design methods of control laws, which is low complexity and independent of accurate mathematical model, is more appropriate. The contributions of this study are summarized as follows:

- A novel integral sliding mode control architecture is proposed based on the TDE technique and modified STA-based compensation algorithm for active suspension systems. Unlike the existing suspension control methods, the presented control scheme can guarantee finite-time stability of the closed-loop system for realizing a simple model-free control method. Moreover, the suspension dynamics of suspensions could be obtained by the TDE information without using the complex modeling or system identification technologies. The modified STA-based compensation algorithm is to provide robustness with respect to bounded model uncertainties/disturbances and finite-time convergence.
- The presented method also possesses an advantage in high computational efficiency, which is relatively easy to implement in practical application. It is because the principal factors influencing the vehicle vertical dynamic performance is the vehicular disturbances, such as the road roughness, unmodeled dynamics and aerodynamic load force, which are difficult to be exactly described. And even if they can be outlined and described, there always requires a large amount of computation. However, the TDE technique makes use of an ingenious method to estimate the plant dynamics, namely,

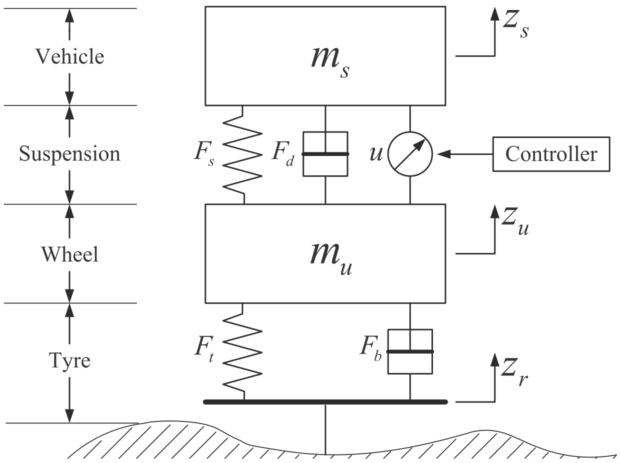

Fig. 1. The active suspension diagram.

through the application of time-delay information rather than the real-time computation of the model dynamics. This is an effectiveness way with high computational efficiency and robustness due to the computation of TDE requires neither the whole dynamic model of suspension nor the vehicular disturbance models.

The paper is organized as follows. In Section 2, the system description and problem formulation of the active suspension system are given. Section 3 analyzes the deficiencies of the classical model-free approach to design of active suspension controller. Section 3 proposes the novel model-free motion control method for active suspensions. In Section 4, experimental validations are conducted. Some conclusions are given in the end.

2. System description and problem formulation

The schematic model of a quarter-car suspension described the vertical dynamics is shown in Fig. 1, which consists of two masses, passive suspension components and an active actuator providing control force [13,35]. Particularly, the sprung mass m_s and the unsprung mass m_u are coupled by an active actuator u with a optimized passive components, i.e., a nonlinear stiffness spring F_s, a nonlinear damper F_d. The tyre can also be described as a spring F_t together with a damper F_b. z_s and z_u denote the vertical displacements of the sprung and unsprung mass, respectively. z_r is the road input.

The vertical dynamics of a quarter-car suspension may be characterized as

$$\begin{aligned} m_s\ddot{z}_s &= -F_s(z_s, z_u) - F_d(\dot{z}_s, \dot{z}_u) + u + F_\Delta \\ m_u\ddot{z}_u &= F_s(z_s, z_u) + F_d(\dot{z}_s, \dot{z}_u) - F_t(z_u, z_r) - F_b(\dot{z}_u, \dot{z}_r) - u \end{aligned} \tag{1}$$

where F_Δ denotes the approximate expression of the model uncertainty or external disturbance term contained in the sprung dynamic. In general, F_Δ is an efficient way to describe the variations of the static load. In practical application, the change rate of the lumped disturbance F_Δ is assumed to be bounded.

Numerous significant studies of active suspensions are based on the model (1). However, due to the fact that the practical active suspension model contains several nonlinear properties and unknown uncertainties, the precise mathematical model in vehicle industry is difficult to obtained, or the costs are greater to identify the suspension model. Therefore, for the active suspension system (1), is it possible to design a controller without using the identified suspension model? In other words, how to design a model-free control method for the active suspension to improve the superior vehicle performance is the key objective of this study.

To address the above-mentioned issue, inspired by [2,21,26], the drawback of the classical model-free control, namely, feedback linearization control with the ESO, is analyzed firstly, and then a novel model-free control scheme is proposed for the active suspension system to improve the control performance. Thus, the problem statement of this paper can be summarized as follows. For active suspension systems, the primary objective of this paper is to synthesize a control law u which can effectively reduce the vertical vibration of the vehicle body and isolate the vibration force transmitted to the passengers, and meanwhile the basic suspension constraints of structures are also ensured.

3. Revisit of the feedback linearization control with the ESO

To construct the unknown dynamic information of the suspension system (1), the unknown term can be calculated as follows

$$F_s(z_s, z_u) + F_d(\dot{z}_s, \dot{z}_u) - F_\Delta = u - m_s\ddot{z}_s \tag{2}$$

During implementing process, if the right-hand parameters of (2) are known, it will lead to the algebraic loops and cannot be achieved when the algorithm (2) is applied directly. To address this problem, several methods based on observers have been presented to estimate the unknown information as reviewed in [36]. The ESO is such an observer in which the unknown information can be estimated using the input and output data from the plant [21].

By introduce a nominal parameter $\bar{m}_s$, which is an crude estimation of the true parameter of m_s. Then, the dynamic equation of the suspension (1) can be rearranged as

$$u = \bar{m}_s \ddot{z}_s + \psi \tag{3}$$

where ψ is treated as a generalized disturbance term including all unknown dynamics and disturbances given by

$$\psi = (m_s - \bar{m}_s)\ddot{z}_s + F_s(z_s, z_u) + F_d(\dot{z}_s, \dot{z}_u) + F_\Delta \tag{4}$$

The system tracking errors for the suspension (3) are defined as

$$\begin{aligned} z_1 &= z_s - z_d \\ z_2 &= \dot{z}_1 = \dot{z}_s - \dot{z}_d \end{aligned} \tag{5}$$

where z_d is the desired reference trajectory with second order differentiable, it and its derivative are both bounded.

Thus, the control objective is to construct a controller u such that the tracking errors z_1, z_2 converge to a small neighborhood of zero with the initial data $z_0 = (z_{10}, z_{20})^T \in \mathbb{R}^2$.

As the control law employed in [21], it can extend ψ as an extended system state variable, namely, define $z_3 = -\frac{1}{\bar{m}_s}\psi$, and its time derivative $h(t)$. Hence, the error dynamics of (3) can be described as

$$\begin{aligned} \dot{z}_1 &= \quad z_2 \\ \bar{m}_s \dot{z}_2 &= \quad u - \bar{m}_s \ddot{x}_d + \bar{m}_s z_3 \\ \dot{z}_3 &= \quad h(t) \end{aligned} \tag{6}$$

Based on the above extended system model (6), a linear ESO is constructed as [21]

$$\begin{aligned} \dot{\hat{z}}_1 &= \quad \hat{z}_2 + 3\omega_0(z_1 - \hat{z}_1) \\ \bar{m}_s \dot{\hat{z}}_2 &= \quad u - \bar{m}_s \ddot{x}_d + \bar{m}_s \hat{z}_3 + 3\bar{m}_s \omega_0^2 (z_1 - \hat{z}_1) \\ \dot{\hat{z}}_3 &= \quad \omega_0^3 (z_1 - \hat{z}_1) \end{aligned} \tag{7}$$

where $\hat{z} = [\hat{z}_1, \hat{z}_2, \hat{z}_3]^T$ denotes the state estimate and $\omega_0 > 0$ is the bandwidth of the ESO. Define the estimation error $\tilde{z}_i = z_i - \hat{z}_i,\ i = 1, 2, 3$. According to (6) and (7), the error dynamics of the observer can be described as

$$\dot{\tilde{z}}_1 = \tilde{z}_2 - 3\omega_0 \tilde{z}_1 \dot{\tilde{z}}_2 = \tilde{z}_3 - 3\omega_0^2 \tilde{z}_1 \dot{\tilde{z}}_3 = h(t) - \omega_0^3 \tilde{z}_1 \tag{8}$$

It is shown in [21] that if $h(t)$ is bounded, the estimated errors are commonly bounded by positive constants ϵ_i after a finite time T_1, i.e.,

$$|\tilde{z}_i| \leqslant \epsilon_i, \epsilon_i = O\left(\frac{1}{\omega_0^c}\right); \quad i = 1, 2, 3,\ \forall t \geqslant T_1 \tag{9}$$

where c is some positive integer. This result indicates that the estimated errors of the ESO are bounded and their upper bounds monotonously decrease with the increase of the bandwidth parameter ω_0. Thus, to achieve the desired control performance, the estimated state $\hat{z}_3$ can be used to describe the extended term z_3. Furthermore, a feedback linearization control law with ESO is given by

$$u = \bar{m}_s(-c_1 z_1 - c_2 z_2) + \bar{m}_s \ddot{x}_d - \bar{m}_s \hat{z}_3 \tag{10}$$

Then, the closed-loop system of (6) can be written as

$$\begin{aligned} \dot{z}_1 &= \quad z_2 \\ \dot{z}_2 &= \quad -c_1 z_1 - c_2 z_2 + \tilde{z}_3 \end{aligned} \tag{11}$$

Remark 1. According to the analysis in [21], the error states z_1, z_2 in (11) can realize an exponentially converging transient performance and the steady state-error can be adjusted by increasing gain c_1, c_2 and/or ω_0. However, increasing these gains will result in the need for increased bandwidth of the closed-loop system. As explained earlier, high gain/bandwidth of the controller and observer may be impractical in control practice since the existence of the measurement noise and unknown unmodeled dynamics of the suspension systems. Hence, the suspension performance is limited using the control law (10) in practical applications. The uncompensated residual estimate errors in this control law is another problem that may directly influence the control precision, and even result in performance degradation when the estimated errors could not be neglected simply. In addition, this algorithm can only guarantee the asymptotic convergence, which still has plenty of scope for further improve the dynamic response. Different from the asymptotic stability, finite-time stability can realize superior robustness performance with rapid dynamic response.

To overcome the drawback of the abovementioned method and to make the model-free control strategy more suitable from the viewpoint of implementation, the following TDE-based integral sliding mode control with an additional continuous disturbance compensation is proposed in the next Section of this paper. This technique could eliminate the evaluated errors in a finite-time, avoid this type of high gain/bandwidth issue, and the suspension dynamic behavior is considered as the nominal system without unknown information to design any nominal control law.

4. Proposed continuous integral like SMC with TDE

4.1. Controller derivation

In this paper, unlike the design method of ESO, the generalized disturbance term of (3) is estimated based on the TDE technique, which is attributed to its advantages of easy realization, fast modeling and relatively satisfactory precision. The following mathematical formulation of design processes explains this design method in detail.

First, the estimate of ψ in (4) is defined as $\hat{\psi}$, which can be obtained by the TDE approach, i.e., one sample-delayed measurement of $\psi(t)$. Thus, in view of (3), the estimation $\hat{\psi}$ can be expressed by

$$\hat{\psi}(t) = \psi(t-L) = u(t-L) - \bar{m}_s\ddot{z}_s(t-L) \tag{12}$$

where L is a sampling time period. It is notable that the estimated results $\hat{\psi}(t)$ by use of this algorithm approximate well to real ones $\psi(t)$ and the estimated errors can be sufficient close to zero if the sampling time L is sufficiently small. These situations, while justified on principle, can not accurately estimate the generalized dynamic $\psi(t)$ even for small sampling period L in practice. As mentioned earlier, the existence of the TDE errors, namely, the error between $\hat{\psi}(t)$ and $\psi(t)$, is inevitable since almost all practical control systems are affected by a limited sample frequency, measurement noise, together with hard nonlinearity [26]. Hence, it is essential to restrain the TDE errors via a special compensative control strategy.

In the following analysis, consider again the error variables (5), but now constructing the following control law for the suspension (3) as

$$u = m_s(u_n + u_c) \tag{13}$$

where u_n is a nominal control law to realize the desired superior performance without disturbance, and u_c is a continuous error compensator to deal with the TDE estimated errors. It is worth noting that u_n can be designed separately from u_c.

Based on the estimation $\hat{\psi}$ in (12) and error variable (5), a sliding surface is then selected as follows:

$$\sigma = z_2 - z_{20} - \int_0^t \left(-\frac{1}{\bar{m}_s}\hat{\psi} - \ddot{z}_d + u_n\right)dt \tag{14}$$

where z_{20} is the initial data of z_2, u_n in (14) is determined for guaranteeing the finite-time stability and given later.

The time derivative of σ along the closed-loop system is given by

$$\bar{m}_s\dot{\sigma} = u - \psi + \hat{\psi} - \bar{m}_s u_n = \bar{m}_s u_c - \psi + \hat{\psi} \tag{15}$$

where the Eq. (13) is used. To facilitate the analysis, define the estimation error of the generalized term ψ as

$$\omega \triangleq \psi - \hat{\psi} = \omega_1 + \omega_2 \tag{16}$$

where ω_1 represents the non-differential error terms, and ω_2 is the differential ones.

Substituting (16) into (15), it can be derived that

$$\dot{\sigma} = u_c - \frac{1}{\bar{m}_s}\omega \tag{17}$$

In the classical STA [37], the corrective term is given by

$$u_c(t) = -c_3|\sigma(t)|^{\frac{1}{2}}\mathrm{sign}(\sigma(t)) - c_4\int_0^t \mathrm{sign}(\sigma(\tau))d\tau \tag{18}$$

where c_3 and c_4 are positive constants. Through the analysis of the correction term (18), it is not difficult to find that the transient state trajectories of this algorithm are very slow when they are away from the origin due to the boundness of the signum function in (18). Thus, a slightly modified method by the addition of linear terms is introduced to improve the convergence performance of the algorithm [34]. The modified STA is chosen as

$$u_c(t) = -c_3\varphi_1(\sigma(t)) - c_4\int_0^t \varphi_2(\sigma(\tau))d\tau \tag{19}$$

where

$$\varphi_1(\sigma(t)) = \sigma(t) + c_5|\sigma(t)|^{\frac{1}{2}}\mathrm{sign}(\sigma(t)) \tag{20}$$

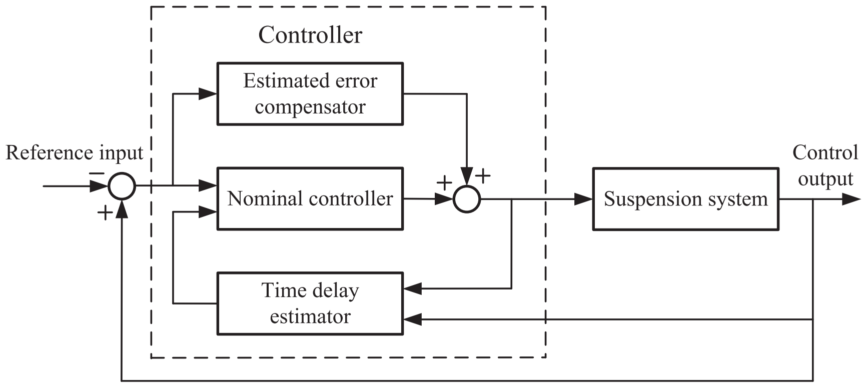

Fig. 2. Overall control structure.

$$\varphi_2(\sigma(t)) = \varphi_1'(\sigma(t))\varphi_1(\sigma(t)) = \sigma(t) + \frac{c_5^2}{2}\mathrm{sign}(\sigma(t)) + \frac{3}{2}c_5|\sigma(t)|^{\frac{1}{2}}\mathrm{sign}(\sigma(t)) \tag{21}$$

where c_3, c_4 and c_5 are appropriately selected positive parameters. The first term $c_3\varphi_1(\sigma(t))$ in (19) is mainly focuses on improving the rate of convergence when the states of this method are away from the origin. The parameters c_4 and c_5 are applied in achieving desired finite-time convergence performance and restraining influence on uncertainties of the plant. In addition, based on the analysis in [38,13,39], we can conclude that the change rate of the TDE error ω satisfies the following inequalities

$$\begin{aligned} |\omega_1| \leqslant & \quad \bar{m}_s\delta_1|\varphi_1(\sigma)| \\ \left|\tfrac{d}{dt}\omega_2\right| \leqslant & \quad \bar{m}_s\delta_2|\varphi_2(\sigma)| \end{aligned} \tag{22}$$

where $\delta_1 \geqslant 0$ and $\delta_2 \geqslant 0$ are some known constants.

Finally, the disturbance is estimated by (19) and compensated when the states reach the sliding surface. Under the condition without disturbance, the nominal controller u_n is given by

$$u_n = -c_1|z_1|^{\alpha_1}\mathrm{sign}(z_1) - c_2|z_2|^{\alpha_2}\mathrm{sign}(z_2) + \frac{1}{\bar{m}_s}\hat{\psi} + \ddot{z}_d \tag{23}$$

where c_i and α_i $(i = 1, 2)$ are positive constants. c_i are to be designed such that the polynomial $p^2 + c_2p + c_1 = 0$, which corresponds to system (23), is Hurwitz. α_1 and α_2 satisfy

$$\alpha_1 = \frac{\alpha_2}{2 - \alpha_2} \tag{24}$$

with $\alpha_2 \in (0, 1)$.

With the above presented model-free finite-time controller, the results for the suspension (1) now establish the following theorem. Specially, Fig. 2 describes the overall control structure of the proposed control scheme.

4.2. Stability analysis

Theorem 1. *Consider the TDE defined as (12) for the active suspension system in (1) with the tracking errors (5). There exist positive design parameters c_i, α_1 and α_2 for $i = 1, \ldots, 5$, such that the suspension (1) can achieve finite-time stability under the model-free control law designed as (13) with the sliding mode surface σ defined by (14), the nominal controller u_n and the disturbance compensator u_c, respectively, selected as (23) and (19), if the error terms are finite-time estimated with the condition (22).*

Proof. The following two steps contribute to proving the main results. The first step concentrates on proving $\sigma = \dot{\sigma} = 0$ in a finite time with the estimated error term. Then, it will show that the nominal control law governs the closed-loop suspension when the estimated error term is compensated by the error compensator.

Step 1: Selecting a Hurwitz matrix $\mathcal{A}$ as

$$\mathcal{A} = \begin{bmatrix} -c_3 & 1 \\ -c_4 & 0 \end{bmatrix} \tag{25}$$

where $c_3 > 0$ and $c_4 > 0$. Substituting (19) into (17) results in

$$\begin{aligned}\dot{\sigma} &= \varsigma - c_3\varphi_1(\sigma(t)) - \frac{1}{\bar{m}_s}\omega_1 \\ \dot{\varsigma} &= -c_4\varphi_2(\sigma(t)) - \frac{1}{\bar{m}_s}\frac{d}{dt}\omega_2\end{aligned} \tag{26}$$

with $\varsigma = -\frac{1}{\bar{m}_s}\omega_2 - c_4\int_0^t \varphi_2(\sigma(\tau))d\tau$. Let the $\eta = [\varphi_1(\sigma) \quad \varsigma]^T$ be the augmented state vector. Then, to perform the stability analysis, this study chooses the Lyapunov function $V(\sigma,\varsigma) = \eta^T\mathcal{P}\eta$ with $\mathcal{P} = \mathcal{P}^T = \begin{bmatrix}\mu+4\epsilon^2 & -2\epsilon \\ -2\epsilon & 1\end{bmatrix}$, $\mu > 0$ and $\epsilon > 0$. It is noteworthy that the function $V(\sigma,\varsigma)$ is continuous and differentiable almost everywhere, except the subspace on $S = \{(\sigma,\varsigma) \in \mathbb{R}^2 | \sigma = 0\}$.

The time derivative of $\varphi_1(\sigma(t))$ can be formulated as

$$\varphi_1'(\sigma(t)) = \frac{d\varphi_1}{d\sigma} = \frac{1}{2|\sigma|^{1/2}} + c_5 \tag{27}$$

then, the $\varphi_2(\sigma(t))$ can also be expressed by

$$\varphi_2(\sigma(t)) = \varphi_1'\varphi_1 = \left(\frac{1}{2|\sigma|^{1/2}} + c_5\right)\varphi_1 \tag{28}$$

Now, taking the derivative of the variable η yields

$$\dot{\eta} = \begin{bmatrix}\varphi_1'(\sigma)\left(-c_3\varphi_1(\sigma(t)) + \varsigma - \frac{1}{\bar{m}_s}\omega_1\right) \\ -c_4\varphi_2(\sigma(t)) - \frac{1}{\bar{m}_s}\frac{d}{dt}\omega_2\end{bmatrix} = \varphi_1'(\sigma)\mathcal{A}\eta + \varpi \tag{29}$$

with $\varpi = \begin{bmatrix}-\varphi_1'(\sigma)\frac{1}{\bar{m}_s}\omega_1 \\ -\frac{1}{\bar{m}_s}\frac{d}{dt}\omega_2\end{bmatrix}$, in which the derivative exists in $\mathbb{R}^2 \setminus S$.

Hence, the derivative of $V(\sigma,\varsigma)$ on the same subset can then be computed as

$$\dot{V}(\sigma,\varsigma) = \dot{\eta}^T\mathcal{P}\eta + \eta^T\mathcal{P}\dot{\eta} = \varphi_1'(\sigma)\eta^T\left(\mathcal{A}^T\mathcal{P} + \mathcal{P}\mathcal{A}\right)\eta + 2\eta^T\mathcal{P}\varpi = -\varphi_1'(\sigma)\eta^T\mathcal{Q}\eta + 2\eta^T\mathcal{P}\varpi \tag{30}$$

with

$$\mathcal{Q} = -\left(\mathcal{A}^T\mathcal{P} + \mathcal{P}\mathcal{A}\right) = \begin{bmatrix}2c_3\mu + 4\epsilon(2\epsilon c_3 - c_4) & * \\ c_4 - 2\epsilon c_3 - \mu - 4\epsilon^2 & 4\epsilon\end{bmatrix} = \begin{bmatrix}2c_3\mu - 4\epsilon\mu & * \\ -4\epsilon^2 & 4\epsilon\end{bmatrix} \tag{31}$$

where the gains c_3 and c_4 are selected as (32) and (33), similar to [37,34], to obtain (31) and to ensure the positive definiteness of matrix $\mathcal{Q}$,

$$c_3 \geqslant \delta + \frac{1}{\mu}\left(\frac{1}{4\epsilon}(4\epsilon^2 + 2\epsilon\delta_1 + \delta_2)^2 + 2\epsilon(\delta_2 + \mu) + \epsilon + \delta_1(\mu + 4\epsilon^2)\right) \tag{32}$$

$$c_4 = \mu + 2\epsilon c_3 \tag{33}$$

with $\delta > 0$ being arbitrary positive constant.

In addition, based on (22), $\eta^T\mathcal{P}\varpi$ is calculated as

$$\begin{aligned}\eta^T\mathcal{P}\varpi &= -\frac{1}{\bar{m}_s}\left[\left((\mu+4\epsilon^2)\varphi_1 - 2\epsilon\varsigma\right)\varphi_1'\omega_1 - (-2\epsilon\varphi_1(\sigma) + \varsigma)\frac{d}{dt}\omega_2\right] \\ &\leqslant \frac{1}{\bar{m}_s}\left[(\mu+4\epsilon^2)\varphi_1'|\varphi_1||\omega_1| + 2\epsilon\varphi_1'|\varsigma||\omega_1| + (2\epsilon|\varphi_1| + |\varsigma|)\left|\frac{d}{dt}\omega_2\right|\right] \\ &\leqslant \varphi_1'\left(\left(\delta_1(\mu+4\epsilon^2) + 2\epsilon\delta_2\right)|\varphi_1|^2 + (\delta_2 + 2\epsilon\delta_1)|\varsigma||\varphi_1|\right)\end{aligned} \tag{34}$$

Thus, it is deduced that $2\eta^T\mathcal{P}\varpi \leqslant \varphi_1'\bar{\eta}^T\Gamma\bar{\eta}$, where $\Gamma = \begin{bmatrix}2\delta_1(\mu+4\epsilon^2) + 4\epsilon\delta_2 & * \\ \delta_2 + 2\epsilon\delta_1 & 0\end{bmatrix}$ and $\bar{\eta} = [|\varphi_1|, |\varsigma|]^T$. By means of the inequality $\eta^T\mathcal{P}\eta \geqslant \bar{\eta}^T\mathcal{P}\bar{\eta}$, it results in

$$\dot{V}(\sigma,\varsigma) \leqslant -\varphi_1'(\sigma)\bar{\eta}^T\bar{\mathcal{Q}}\bar{\eta} \tag{35}$$

where $\bar{\mathcal{Q}} = \mathcal{Q} - \Gamma$ and

$$\bar{\mathcal{Q}} - 2\epsilon I = \begin{bmatrix}2c_3\mu - 2\delta_1(\mu+4\epsilon^2) - 4\epsilon(\mu+\delta_2) - 2\epsilon & * \\ -(4\epsilon^2 + \delta_2 + 2\epsilon\delta_1) & 2\epsilon\end{bmatrix}$$

By selecting c_3 as in (32), it can guarantee the matrix $\bar{\mathcal{Q}} - 2\epsilon I$ be positive definite. Therefore,

$$\dot{V}(\sigma,\varsigma) \leqslant -\left(\frac{1}{2|\sigma|^{1/2}} + c_5\right)2\epsilon\|\bar{\eta}\|^2 \tag{36}$$

where $\|\bar{\eta}\|^2 = \|\eta\|^2$, and

$$\|\eta\|^2 = |\varphi_1|^2 + |\varsigma|^2 = |\sigma| + 2c_5|e|^{3/2} + c_5^2|\sigma|^2 + |\varsigma|^2 \tag{37}$$

is the Euclidean norm of η. Furthermore, based on

$$\lambda_{\min}\{\mathcal{P}\}\|\eta\|^2 \leqslant \eta^T\mathcal{P}\eta \leqslant \lambda_{\max}\{\mathcal{P}\}\|\eta\|^2 \tag{38}$$

and

$$|\sigma|^{1/2} \leqslant \|\eta\| \leqslant \frac{V^{\frac{1}{2}}(\sigma,\varsigma)}{\lambda_{\min}^{\frac{1}{2}}\{\mathcal{P}\}} \tag{39}$$

it can conclude that

$$\dot{V}(\sigma,\varsigma) \leqslant -\kappa_1 V^{\frac{1}{2}}(\sigma,\varsigma) - \kappa_2 V(\sigma,\varsigma) \tag{40}$$

where

$$\kappa_1 = \frac{\epsilon\lambda_{\min}^{\frac{1}{2}}\{\mathcal{P}\}}{\lambda_{\max}\{\mathcal{P}\}}, \quad \kappa_2 = \frac{2\epsilon c_5}{\lambda_{\max}\{\mathcal{P}\}}. \tag{41}$$

According to the Theorem 2 in [40], it can be observed that the trajectories of (26) are finite-time stable, namely, the states of (26) beginning in initial data $\sigma(t_0), \varsigma(t_0) \in \mathbb{R}^2$ could reach the equilibrium point $(\sigma,\varsigma) = 0$ in a finite-time

$$T(\sigma(t_0)) = \frac{2}{\kappa_2}\ln\left(\frac{\kappa_1 + \kappa_2 V^{\frac{1}{2}}(\sigma(t_0),\varsigma(t_0))}{\kappa_1}\right) \tag{42}$$

where t_0 is the initial instance.

Step 2: The result of step 1 further implies that $\dot{\sigma} = 0$. Hence, when the sliding mode is reached, the TDE error is obtained by

$$\bar{m}_s u_c = \omega \tag{43}$$

which indicates that the error terms are eliminated from the suspension (3) if the states arrive at the sliding manifold in a finite time. Therefore, the error compensator u_c provides an effective method to implement error compensation. As analyzed in [30], it can conclude that the trajectories of the system (3) cannot escape to infinity in finite time.

By substituting (43) and (23) into the suspension (3), it can obtain the following dynamic system without disturbance

$$\begin{cases} \dot{z}_1 = z_2 \\ \dot{z}_2 = -c_1|z_1|^{\alpha_1}\operatorname{sign}(z_1) - c_2|z_2|^{\alpha_2}\operatorname{sign}(z_2) \end{cases} \tag{44}$$

which means that the closed-loop active suspension is controlled by u_n if the tracking error states on the sliding manifold. Thus, consider a positive-definite Lyapunov function $V = \frac{c_1}{\alpha_1+1}|z_1|^{\alpha_1+1} + \frac{1}{2}z_2^2$, which time derivative along (44) is $\dot{V} = c_1|z_1|^{\alpha_1}\operatorname{sign}(z_1)\dot{z}_1 + z_2\dot{z}_2$. By substituting (44) into the above equation, one has $\dot{V} = -c_2|z_2|^{1+\alpha_2}$. Hence, it can conclude that $\dot{V}$ is a negative semi-definite while the original function is a positive-definite. According to LaSalle's invariance principle [41], it can obtain $z_1 \to 0$ and $z_2 \to 0$ as $t \to \infty$ for any initial data. Therefore, we can conclude that z_1 and z_2 are global asymptotic converge to zero. Note that $(z_1, z_2) = (0, 0)$ is the equilibrium of (44). Based on the Definition 2 in [2], system (44) is homogeneous with a degree $\tau = (\alpha_1 - 1)/2 < 0$ relative to $(\vartheta_1, \vartheta_2) = (1, (\alpha_1 + 1)/2)$. Thus, by means of Lemma 1 in [2] and the finite-time separate principle, the whole system is finite-time stable.

In addition, active suspension system (1) is a forth-order system, while the controller design procedure is aim at the second-order tracking error dynamics. All the remained two states of the suspension system constitute the zero dynamics subsystem. The detailed zero dynamics characteristics of the active suspension is omitted here due to the similar analysis procedure as in [30].

This completes the proof. □

Remark 2. The classical Lyapunov theorem could not be introduced to analyze the stability of the system directly because the candidate function $V(\sigma,\varsigma)$ is not locally Lipschitz but continuous. Nevertheless, it can demonstrate that $V(\sigma,\varsigma)$ is an absolutely continuous function with respect to the system states, and thus it decreases monotonically if $\dot{V}$ is negative definite almost everywhere. Thus, the solutions of (26) should be understood in Filippov sense [42].

Remark 3. By comparing with the results of (11) and (44), it can be found that the suspension dynamics have been obviously improved for both transient and steady-state responses, that is, the closed-loop system is finite-time stable rather than bounded stable, and the error terms can be eliminated completely using the corresponding compensation technique. Thus, the proposed control method could achieve an excellent performances with the condition of model-free.

5. Comparative experimental studies

The performance of the proposed control structure is evaluated in experiments using the active suspension setup as shown in Fig. 3. This setup simulates a quarter-car suspension in the laboratory, whose model data are shown in Table 1. Moreover, comparison between the following three situations are carried out to investigate the effectiveness of the proposed control system.

- S1: The passive suspension system.
- S2: The feedback linearization control law in (10) with ESO in (7). The controller parameters are given by $c_1 = 400, c_2 = 20, \omega_0 = 150$, and $\bar{m}_s = 2.2$.
- S3: The proposed model-free finite time control law. The controller parameters are chosen as $c_1 = 25, c_2 = 10$ $c_3 = 0.4, c_4 = 0.6, c_5 = 0.5, \alpha_1 = 9/23, \alpha_2 = 9/16$, and $\bar{m}_s = 2.2$.

In order to provide a comfortable riding performance, the desired reference trajectory is always set as zero at normal road condition during experiment, i.e., $z_d = 0$. In this study, it is important for the vertical sprung response to track the desired value to improve the suspension performances. Here, one can determine the resonant frequency of the suspension setup is about 3 Hz. Thus, the presented control law is verified by sinusoidal road disturbed input with frequency 3 Hz and amplitude 0.2cm, namely, $z_r = 0.002\sin(6\pi t)$.

Fig. 4 depicts the experimental results under the sinusoidal road excitation. This figure illustrates the closed-loop output responses of the vertical displacement z_s, where the two active control performances are compared with S1. According to Fig. 4, the proposed S3 controller had the best vibration isolation capability because it managed to produce the fast output

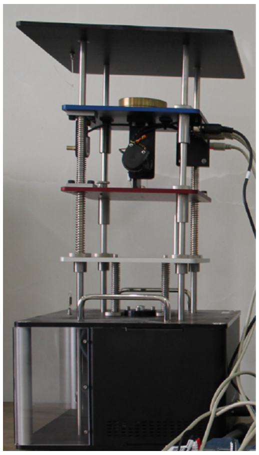

Fig. 3. The active suspension setup.

Table 1
Parameter description of the suspension.

Parameter	Value	Meaning
m_s	2.45 kg	Mass of sprung
m_u	1 kg	Mass of unsprung
k_s	900 N/m	Linear stiffness coefficient of spring
k_{s_n}	10 N/m^3	Nonlinear stiffness coefficient of spring
b_e	8 Ns/m	Extension damping coefficient of damper
b_c	7 Ns/m	Compression damping coefficient of damper
k_f	2500 N/m	Stiffness coefficients of tire
b_f	5 Ns/m	Damping coefficient of tire

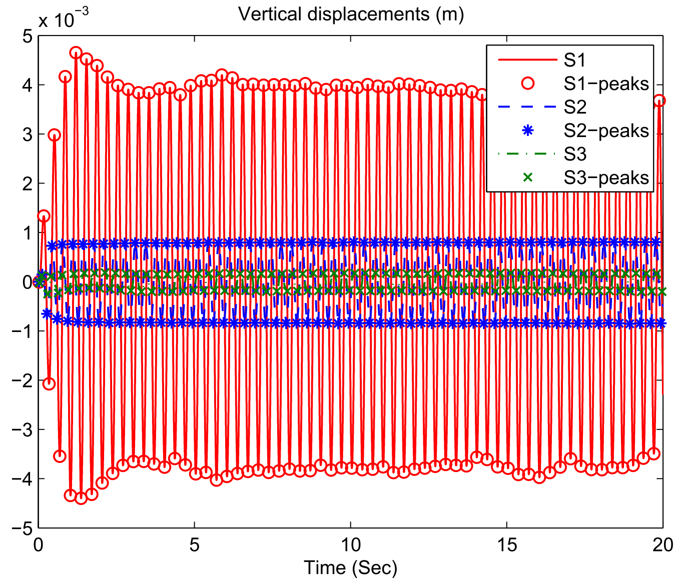

Fig. 4. Vertical displacement responses.

responses with the finite-time controller and the disturbance compensation, and it can effectively improve the suspension performances in the existence of external disturbances. Moreover, the magnitude of the displacement in S3 is about 10 times smaller than S1, which illustrates the effectiveness of the proposed S3. Additionally, it is not difficult to find out that the dynamic control performance of S2 and S3 can both suppress the disturbances and achieve a rather good suspension performances. However, the final performance of S2 based on the asymptotic stability is worse than S3 based on the finite-time concept. These results illustrate the advantage of the present control method.

One of the important purposes of suspension systems is to improve the ride comfort by attenuating the vehicle vibration since the ride comfort is closely connected with the body acceleration. Thus, for comparing performances of the three suspension systems, Fig. 5 shows the vertical acceleration responses. As for the peak value, S2 and S3 have both reduced the vibration compared with S1. Moreover, the performance of S3 is considerably better than that in S2. These results illustrate the presented controller is an effective approach for enhancing the suspension performance.

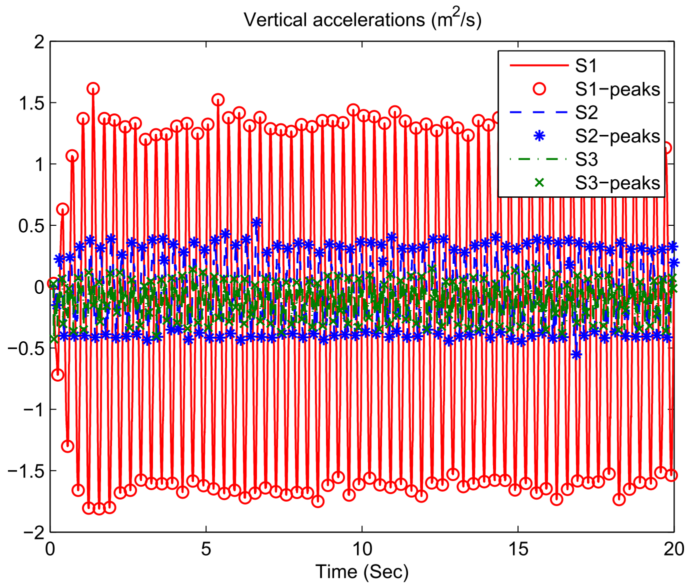

Fig. 5. Vertical acceleration.

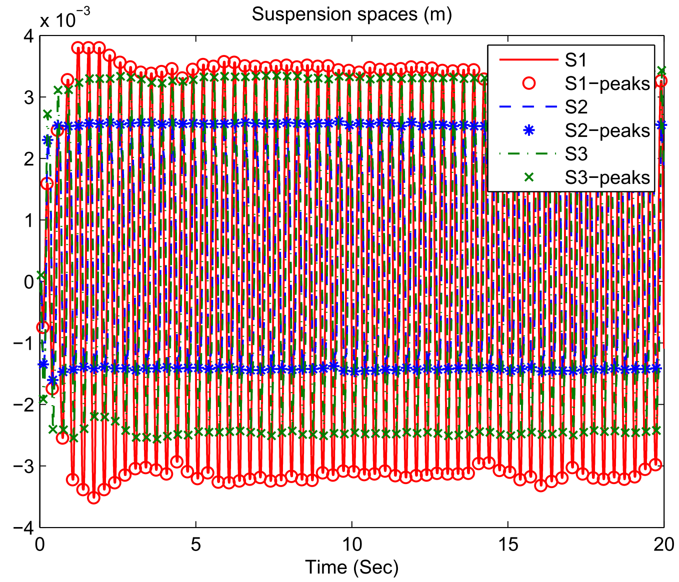

Fig. 6. Suspension spaces.

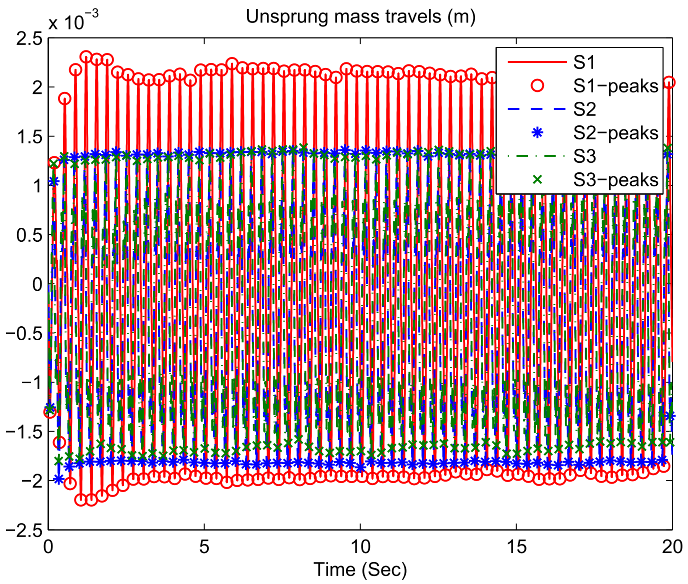

Fig. 7. The responses of unsprung mass displacement $z_u - z_r$.

Additionally, considering the physical constraint of the suspension system, the suspension space should be limited into necessary scope under the road input. In fact, the maximum suspension space of the experimental setup is $z_{\max} = 0.038$m. Thus, from Fig. 6, it can see that the suspension space $z_s - z_u$ of these three suspensions are all at the given range. As it states earlier, the vertical displacement z_s of S3 is smaller than S2, thus, S3 might require some additional space to suppress the isolation and realize an excellent performance. This is also reflected in Fig. 6. That is because the active suspension system is more elastic and efficient to provide the ride quality by both add and dissipate energy from the system. Hence, a comfortoriented suspension calls for a low damping and a large stroke of the chassis mass to provide sufficient isolation. The vibration isolation properties of a suspension can be enhanced by softer primary springs, which allows for too much movement.

The tyre travel responses of the tyre are shown in Fig. 7. In this figure, it can conclude that the active suspensions could enhance the road handling compared with the passive suspension, and S2 and S3 almost have the same level of the performance improvement. Fig. 8 describes the actuator control inputs.

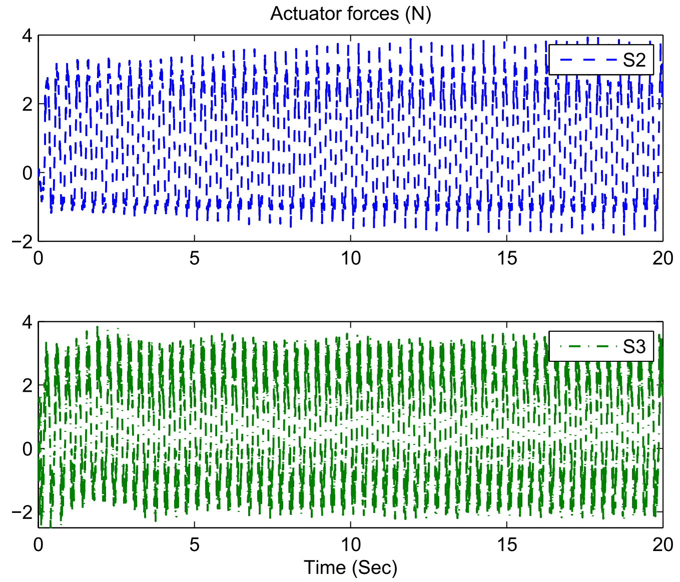

Fig. 8. Control input.

Table 2
The Maximum and RMS values of suspension states.

Types	Vertical displacement $\|z_s\|$		Body acceleration $\|\ddot{z}_s\|$		Suspension space $\|z_s - z_u\|$		Unsprung travel $\|z_u - z_r\|$	
	MAX (m)	RMS (m)	MAX (m/s^2)	RMS (m/s^2)	MAX (m)	RMS (m)	MAX (m)	RMS (m)
S1	0.0047	0.0027	1.8104	1.0047	0.0038	0.0025	0.0023	0.0013
S2	8.5232×10^{-4}	5.7368×10^{-4}	0.5515	0.2275	0.0026	0.0016	0.0020	0.0011
S3	2.5326×10^{-4}	1.3054×10^{-4}	0.4265	0.1399	0.0034	0.0020	0.0018	0.0011

The results of quantitative index analysis for the previous experimental results using root-mean-square value (RMS) are also introduced to describe the degree of suspension performance improvement. It is generally known that the RMS values of the system dynamic outputs are closely related to suspension performance. Therefore, the RMS values are able to describe the quantitative indexes. A computational formula of the RMS for the signal $\xi(t)$ is given by

$$\text{RMS}_{\xi} = \sqrt{\frac{1}{N}\int_0^N \xi^T(t)\xi(t)dt}$$

where $N = 20\text{s}$ is used in computing the RMS values of the vehicle sprung vertical displacement, acceleration, suspension space and the tyre travel.

The following Table 2 tabulates the numerical value of the quantized suspension performances, together with the percentage of performance improvement for active suspensions compared with S1 as shown in Fig. 9. Based on the table and figure given, the desired suspension system performances are accomplished by S3 control method, such as reducing the road disturbance and improving ride comfort, it follows by S2. The results also show that the proposed control strategy is able to improve the vibration isolation performance (reducing z_s) by 94.61% (MAX value) and 95.17% (RMS value) compared to S1 and 70.29% (MAX value) and 77.25% (RMS value) compared to S2 controller. Moreover, for the vertical acceleration $\ddot{z}_s$, the presented S3 is able to reduce 76.44% (MAX value) and 95.17% (RMS value) influence of the external disturbance compared to S1. In addition, the suspension performance constants, i.e., suspension stoke and tyre travel, have also been improved correspondingly with respect to S1, which means that the active suspensions can reduce tire dynamics, which results in enhancing road handling and system security. Thus, it is proven that the S3 with disturbance compensation based system is able to enhance the suspension performance by producing an excellent dynamic responses with minor disturbance effects.

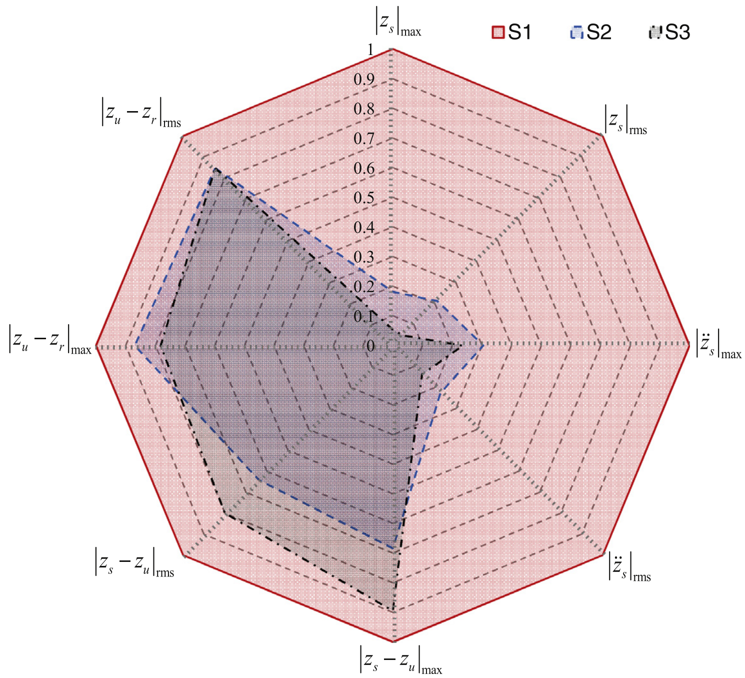

Fig. 9. The percentage of performance improvement with respect to S1.

6. Conclusion

A new finite-time tracking control scheme has been presented for motion control of vehicle suspension system. The control is designed without using the suspension nonlinear dynamics, which could be estimated and canceled by adopting the TDE. Due to the existence of the estimated errors, unlike the traditional signum function-based discontinuous equivalent control term, the proposed estimated error compensator is continuous and finite-time convergent, which is developed based on the modified STA technique and shows a great potential in application to practical vehicle suspensions. The stability of the closed-loop suspension system has been demonstrated in theory under the Lyapunov framework. Owe to the ease of implementation, the effectiveness of the proposed control strategy is verified by conducting experimental studies on an active suspension setup. The experiment results reveal that the presented control law could provide adequate performance as far as decreasing RMS errors of the sprung mass vertical displacement and vertical vehicle acceleration compared with the conversional suspension systems.

Acknowledgements

This work was supported in part by the National Natural Science Foundation of China (61603144), the Natural Science Foundation of Fujian Province (2018J01095), the major Project of Science and Technology Plan of Fujian Province (2013H6016), the Technology Innovation Grant for Middle-Young teachers of Huaqiao University (ZQN-PY509).

References

[1] World Health Organization, Global status report on road safety 2015. http://www.who.int/violenceinjuryprevention/roadsafetystatus/2015/en/ Accessed 10.09.2016.
[2] H. Pan, X. Jing, W. Sun, Robust finite-time tracking control for nonlinear suspension systems via disturbance compensation, Mech. Syst. Signal Process. 88 (2017) 49–61.
[3] D. Ning, S. Sun, H. Du, W. Li, N. Zhang, Vibration control of an energy regenerative seat suspension with variable external resistance, Mech. Syst. Signal Process. 106 (2018) 94–113.
[4] H. Pan, X. Jing, W. Sun, H. Gao, A bioinspired dynamics-based adaptive tracking control for nonlinear suspension systems, IEEE Trans. Control Syst. Technol. 26 (3) (2018) 903–914.
[5] W. Sun, H. Pan, H. Gao, Filter-based adaptive vibration control for active vehicle suspensions with electrohydraulic actuators, IEEE Trans. Veh. Technol. 65 (6) (2016) 4619–4626.
[6] W. Sun, H. Gao, O. Kaynak, Vibration isolation for active suspensions with performance constraints and actuator saturation, IEEE/ASME Trans. Mechatron. 20 (2) (2015) 675–683.

[7] H. Li, X. Jing, H.R. Karimi, Output-feedback-based H_∞ control for vehicle suspension systems with control delay, IEEE Trans. Industr. Electron. 61 (1) (2014) 436–446.
[8] H. Li, X. Jing, H.-K. Lam, P. Shi, Fuzzy sampled-data control for uncertain vehicle suspension systems, IEEE Trans. Cybern. 44 (7) (2014) 1111–1126.
[9] S. Yan, W. Sun, Self-powered suspension criterion and energy regeneration implementation scheme of motor-driven active suspension, Mech. Syst. Signal Process. 94 (2017) 297–311.
[10] H. Ma, H. Liang, Q. Zhou, C.K. Ahn, Adaptive dynamic surface control design for uncertain nonlinear strict-feedback systems with unknown control direction and disturbances, IEEE Trans. Systems, Man, Cybern.: Syst. (2018), https://doi.org/10.1109/TSMC.2018.2855170.
[11] H. Pan, W. Sun, H. Gao, X. Jing, Disturbance observer-based adaptive tracking control with actuator saturation and its application, IEEE Trans. Autom. Sci. Eng. 13 (2) (2015) 868–875.
[12] Y. Zhang, H. Liang, H. Ma, Q. Zhou, Z. Yu, Distributed adaptive consensus tracking control for nonlinear multi-agent systems with state constraints, Appl. Math. Comput. 326 (2018) 16–32.
[13] H. Pan, W. Sun, H. Gao, J. Yu, Finite-time stabilization for vehicle active suspension systems with hard constraints, IEEE Trans. Intell. Transp. Syst. 16 (5) (2015) 2663–2672.
[14] X. Jing, Nonlinear characteristic output spectrum for nonlinear analysis and design, IEEE/ASME Trans. Mechatron. 19 (1) (2014) 171–183.
[15] X.J. Jing, Z.Q. Lang, S.A. Billings, Nonlinear influence in the frequency domain: alternating series, Syst. Control Lett. 60 (5) (2011) 295–309.
[16] Z. Xiao, X. Jing, Frequency-domain analysis and design of linear feedback of nonlinear systems and applications in vehicle suspensions, IEEE/ASME Trans. Mechatron. 21 (1) (2016) 506–517.
[17] J. Han, From PID to active disturbance rejection control, IEEE Trans. Ind. Electron. 56 (3) (2009) 900–906.
[18] J. Yao, Z. Jiao, D. Ma, Extended-state-observer-based output feedback nonlinear robust control of hydraulic systems with backstepping, IEEE Trans. Industr. Electron. 61 (11) (2014) 6285–6293.
[19] J. Yao, Z. Jiao, D. Ma, L. Yan, High-accuracy tracking control of hydraulic rotary actuators with modeling uncertainties, IEEE/ASME Trans. Mechatron. 19 (2) (2014) 633–641.
[20] Z. Gao, Y. Huang, J. Han, An alternative paradigm for control system design, Proceedings of the 40th IEEE Conference on Decision and Control, vol. 5, IEEE, 2001, pp. 4578–4585.
[21] H. Pan, W. Sun, H. Gao, T. Hayat, F. Alsaadi, Nonlinear tracking control based on extended state observer for vehicle active suspensions with performance constraints, Mechatronics 30 (2015) 363–370.
[22] H. Ma, Q. Zhou, L. Bai, H. Liang, Observer-based adaptive fuzzy fault-tolerant control for stochastic nonstrict-feedback nonlinear systems with input quantization, IEEE Trans. Syst., Man, Cybern.: Syst. (2018), https://doi.org/10.1109/TSMC.2018.2833872.
[23] T. Hsia, S. Jung, A simple alternative to neural network control scheme for robot manipulators, IEEE Trans. Industr. Electron. 42 (4) (1995) 414–416.
[24] H. Zhang, Y. Shi, J. Wang, H. Chen, A new delay-compensation scheme for networked control systems in controller area networks, IEEE Trans. Industr. Electron. 65 (9) (2018) 7239–7247.
[25] K. Youcef-Toumi, O. Ito, A time delay controller for systems with unknown dynamics, J. Dyn. Syst. Measure. Control 112 (1) (1990) 133–142.
[26] M. Jin, S.H. Kang, P.H. Chang, Robust compliant motion control of robot with nonlinear friction using time-delay estimation, IEEE Trans. Industr. Electron. 55 (1) (2008) 258–269.
[27] V.I. Utkin, Sliding Modes in Control and Optimization, Springer Science & Business Media, 2013.
[28] H. Zhang, J. Wang, Adaptive sliding-mode observer design for a selective catalytic reduction system of ground-vehicle diesel engines, IEEE/ASME Trans. Mechatron. 21 (4) (2016) 2027–2038.
[29] A. Şabanoviç, Variable structure systems with sliding modes in motion control-a survey, IEEE Trans. Industr. Inf. 7 (2) (2011) 212–223.
[30] H. Pan, W. Sun, Nonlinear output feedback finite-time control for vehicle active suspension systems, IEEE Trans. Industr. Inf. (2018), https://doi.org/10.1109/TII.2018.2866518.
[31] H. Zhang, G. Zhang, J. Wang, H_∞ observer design for lpv systems with uncertain measurements on scheduling variables: Application to an electric ground vehicle, IEEE/ASME Trans. Mechatron. 21 (3) (2016) 1659–1670.
[32] L. Yang, J. Yang, Nonsingular fast terminal sliding-mode control for nonlinear dynamical systems, Int. J. Robust Nonlinear Control 21 (16) (2011) 1865–1879.
[33] A. Levant, Robust exact differentiation via sliding mode technique, Automatica 34 (3) (1998) 379–384.
[34] T. Gonzalez, J.A. Moreno, L. Fridman, Variable gain super-twisting sliding mode control, IEEE Trans. Autom. Control 57 (8) (2012) 2100–2105.
[35] W. Sun, H. Gao, O. Kaynak, Vibration isolation for active suspensions with performance constraints and actuator saturation, IEEE/ASME Trans. Mechatron. 20 (2) (2015) 675–683.
[36] A. Radke, Z. Gao, A survey of state and disturbance observers for practitioners, 2006 American Control Conference (ACC), IEEE, 2006, pp. 5183–5188.
[37] J.A. Moreno, M. Osorio, Strict lyapunov functions for the super-twisting algorithm, IEEE Trans. Autom. Control 57 (4) (2012) 1035–1040.
[38] W. Jue, Z. Jing, Model-free tracking control for vehicle active suspension systems, 2012 34th Chinese Control Conference (CCC), IEEE, 2015, pp. 8067–8072.
[39] V.S. Deshpande, B. Mohan, P. Shendge, S. Phadke, Disturbance observer based sliding mode control of active suspension systems, J. Sound Vib. 333 (11) (2014) 2281–2296.
[40] S. Khoo, L. Xie, S. Zhao, Z. Man, Multi-surface sliding control for fast finite-time leader–follower consensus with high order SISO uncertain nonlinear agents, Int. J. Robust Nonlinear Control 24 (16) (2014) 2388–2404.
[41] J.-J.E. Slotine, W. Li, Applied nonlinear control, vol. 199, Prentice-Hall Englewood Cliffs, NJ, 1991.
[42] A.F. Filippov, Differential Equations with Discontinuous Righthand Sides: Control Systems, vol. 18, Springer Science & Business Media, 2013.